VOL. 15, NO. 1, JANUARY 2020 ISSN 1819-6608
ARPN Journal of Engineering and Applied Sciences

www.arpnjournals.com

SPATIAL AND TEMPORAL VARIATION OF ETO FOR EGYPT USING REMOTE SENSING

Hesham Ezz[1] and Mohamed Abdelwares[2]
[1]Civil Engineering Department, National Research Centre, Dokki, Giza, Egypt
[2]Irrigation and Hydraulics Department, Faculty of Engineering, Cairo University, Egypt
E-Mail: ezz.hisham@gmail.com

ABSTRACT

Egypt is adopting a horizontal agricultural expansion strategy despite facing water scarcity conditions. The agricultural expansion program will be directed towards the uncultivated lands in Egypt which can be estimated to be more than 90% of the total area. Therefore, a sustainable agricultural development is required. The most important component in the agriculture management system is the accurate estimation of the water quantities required for plantation, which is mainly controlled by the evapotranspiration value. The objective of this paper is to calculate the reference evapotranspiration (ETo) over the whole area of Egypt, which is used to calculate the irrigation water consumption, in order to give an insinuation about the suitable areas for the agricultural expansion due to the low evapotranspiration value. The average daily ETo by month is calculated using FAO Penman Monteith equation which is widely recommended due to its detailed theoretical base. The calculated ETo is demonstrated in maps using a GIS environment all over Egypt for each month. The results of ETo showed that the least mean value occurred during December which is about 3.28 mm, while the highest mean value occurred in June and equal to 9.5 mm.

Keywords: reference evapotranspiration, FAO penman Monteith, Egypt, GIS, ETo, remote sensing.

INTRODUCTION

Egypt is now facing water scarcity conditions due to constancy of water resources with increasing in demands. Although this water scarcity situation, the Egyptian government adopted a future strategy for horizontal agricultural expansion, due to the rapid population growth.

Nowadays, the agriculture water demand in Egypt represents about 85% of the total available water [1]. Therefore, the determination of the water quantities for the new irrigated area becomes increasingly important to avoid underestimation or overestimation of crop water consumption.

Two water losses processes define the crop water consumption. The first process is the water loss from the soil surface, wet vegetation, and shallow groundwater is called evaporation (E). The second process is the water loss from the plant tissues, which is called transpiration (T). The combination of these two processes is called evapotranspiration (ET) which represents about 99% of the total water consumptive use of the plant. So, accurate calculation of crop evapotranspiration (ETc) or consumptive water use is significant for water resources planning and irrigation management [2]. The crop evapotranspiration can be calculated using Eq. 1

$$ETc = ETo \times Kc \quad (1)$$

where; ETc is crop evapotranspiration (mm/day), ETo is reference evapotranspiration (mm/day), Kc is crop coefficient. The ETo is defined as the rate of evapotranspiration from a hypothetical reference grass crop cultivated in a land without a shortage in water.

The main factors affecting the reference evapotranspiration (ETo) are location, climatic parameters, management practices and environmental aspects. The main climatic factors affecting evapotranspiration are solar radiation, air temperature, air humidity and wind speed.

There are several physically based methods used for estimating the reference evapotranspiration such as aerodynamic, energy budget and modified penman methods. Also available are several empirical methods for estimating the reference evapotranspiration such as the pan evaporation method.

The most accurate physical model used to calculate the ETo and is considered to be the most reasonable and recommended method in both humid and arid climate regions is the standardized FAO56 Penman-Monteith equation [3, 4, 5].

The FAO56 penman-Monteith equation is used in two well-known applications, i.e. CROPWAT [6] and BISm which is an MS Excel based model [7]. These two applications are friendly users and available as freeware. In the literature there are a lot of researchers used these applications in their studies to calculate the ETo in Egypt [8, 9, 10, 11, 12, 13, 14, 15, 16].

These applications are easy to use, and give the most accurate estimation for the ETo since they are using FAO56 penman-Monteith equation. Those applications are a point calculator, which means they solve for a specific point, but in case of estimating the ETo for hundreds or thousands of points, using such calculator will be time consumer. Most of the studies calculated the ETo for Egypt using these applications represents Egypt in a very few points. For instance, they represent every governorate using one point.

In this paper, the GIS environment is used to integrate the spatial location, climate, terrain, and FAO56 penman-Monteith equation to calculate the average daily ETo by month. The calculated ETo are demonstrated in 12 maps covering Egypt using more than 10,000 points.

MATERIALS AND METHODS

Study area

The ETo is calculated over the whole area of Egypt for the 12 months of the year. Egypt lies in the north-eastern corner of Africa with a total area of one million sq. km. The study area, Egypt, is presented in more than 10,000 points. Figure-1 presents the study area.

Figure-1. The Study area.

ETo calculation

The ETo is calculated using Penman-Monteith equation [17] as presented by Allen et al., 1998 in the United Nations FAO Irrigation and Drainage Paper (FAO 56). The FAO Penman-Monteith equation used to estimate the ETo is presented in Eq. 2 as follows:

$$ETo = \frac{0.408\,\Delta\,(R_n - G) + \gamma\,\frac{900}{T+273}U_2(e_s - e_a)}{\Delta + \gamma\,(1 + 0.34\,U_2)} \quad (2)$$

where; ETo is the reference evapotranspiration [mm/day], Rn is net radiation at the crop surface[MJ/m^2/day], G is soil heat flux density [MJ/m^2/day], T is mean daily air temperature at 2 m height [˚C], U_2 is wind speed at 2 m height [m/s], e_s is saturation vapour pressure [kPa], ea is actual vapour pressure [kPa], (es - ea) is saturation vapour pressure deficit [kPa], Δ is slope of saturation vapour pressure curve [kPa/˚C], and γ is psychrometric constant [kPa/˚C].

The slope of saturation vapour pressure curve at mean air temperature,Δ, is calculated using Eq. 3 as shown below:

$$\Delta = \frac{4098\left[0.6108\exp\left(\frac{17.27\,T}{T+237.3}\right)\right]}{(T+237.3)^2} \quad (3)$$

The psychrometric constant, γ, is calculated using Eq. 4 as follows:

$$\gamma = 0.665 \times 10^{-3}\,P \quad (4)$$

Where P is the atmospheric pressure [kPa] and can be calculated using Eq. 5 as follows:

$$P = 101.3\left(\frac{293 - 0.0065\,z}{293}\right)^{5.26} \quad (5)$$

Where z is the elevation above sea level (m).

The net radiation (Rn) is the net difference between incoming net shortwave radiations (Rns) and the outgoing net longwave radiations. The Rn is calculated using Eq. 6 as shown below:

$$Rn = Rns - Rnl \quad (6)$$

The net shortwave radiations (Rns) resulting from the balance between incoming and reflected solar radiation is given by Eq. 7:

$$Rns = (1 - \alpha)\,Rs \quad (7)$$

Where Rns is the net shortwave radiation [MJ/m^2/d], α is the albedo or canopy reflection coefficient for the reference crop. A fixed value of 0.23 is recommended for the albedo. Rs is the measured incoming solar radiation [MJ/m^2/d].

There are many equations used in the literature to calculate the net long wave radiations (Rnl). In this paper, the equation used is the one proposed by the FAO 56 in [18]. The equation assumes that the rate of longwave energy emission is directly proportional to the absolute surface temperature raised to the fourth power. The equation is expressed in Eq. 8 as follows:

$$R_{nl} = \sigma\left[\frac{T^4_{max,k} - T^4_{min,k}}{2}\right]\left(0.34 - 0.14\sqrt{e_a}\right)\left(1.35\frac{R_s}{R_{so}} - 0.35\right) \quad (8)$$

Where Rnl is net long-wave radiation [MJ/m^2/d], σ is Stefan-Boltzmann constant [4.903 × 10^{-9} MJ/K^4/m^2/d], Tmax,k and Tmin,k are maximum and minimum absolute temperature during the 24-hr period [K], Rs/Rso is the relative shortwave radiation (limited to ≤ 1.0). Rso is the clear sky radiation [MJ/m^2/d] when the actual duration of sunshine equals the maximum daylight hours. The Rso can be calculated using Eq. 9:

$$R_{so} = (0.75 + 2\times10^{-5}z)R_a \quad (9)$$

Where Rso is clear-sky solar radiation [MJ/m^2/d], z is the elevation above sea level [m], and Ra is the extraterrestial radiation [MJ/m^2/d]. The Ra for each day of the year and for different latitudes is calculated from the solar constant, solar declination, and the time of the year as shown in Eq. 10:

$$R_a = \frac{24\times60}{\pi}G_{sc}d_r(\omega_s\sin\varphi\sin\delta + \cos\varphi\cos\delta\sin\omega_s) \quad (10)$$

where, Gsc (0.0820 MJ/m^2/min) is solar constant, dr is inverse relative earth-sun distance Eq. 11, ω_s is the sunset hour angle [rad.] and is expressed in Eq. 12, φ is the latitude [rad.] and is expressed in Eq. 13, and δ is the solar declination [rad.] and is expressed in Eq. 11.

$$d_r = 1 + 0.033 \cos\left(\frac{2\pi}{365} J\right) \quad (11)$$

$$\delta = 0.409 \sin\left(\frac{2\pi}{365} J - 1.39\right) \quad (12)$$

$$\omega_s = \arccos(-\tan\varphi \tan\delta) \quad (13)$$

Where J is the number of the day in the year between January 1st and December 31st. In this paper, the J is calculated at the middle of each month and can be expressed by Eq. 14 as follows:

$$\mathrm{J} = \text{ Integer } (30.4\,\mathrm{Month} - 15) \quad (14)$$

Climate data

In order to obtain the ETo over Egypt using FAO Penman-Monteith equation, some climate data are required. WorldClim Version2 dataset [19] was used, in order to provide the required climate data as the maximum and minimum temperature, radiation, vapor pressure, and wind speed. The monthly average climate data is aggregated across a target temporal range of 1970-2000. Global climate layers of the WorldClim Version2 were used with a spatial resolution of ten minutes.

Digital elevation model

Digital elevation model (DEM) is a digital representation of the surface elevation topography. The DEM of Egypt used has a resolution of 1-arc second (~30 m) and its geo-reference is UTM WGS84 36 N. The DEM is extracted using ArcGIS with Spatial Analyst Extension, from ALOS World 3D - 30m (AW3D30) version 2.1 released in April 2018 [20]. The DEM is essential to calculate the ground elevation for each point in the study area.

RESULTS AND DISCUSSIONS

ETo maps

The average daily ETo values by month are calculated by FAO Penman-Monteith equation described before using the climate, spatial location, and terrain data for more than 10,000 points covering Egypt. The ArcMap software as a GIS environment is used for calculating the average monthly ETo. The Natural Neighbor method is applied using the calculated ETo to create an average daily ETo for each month as demonstrated in Figure-2, Figure-3, and Figure-4.

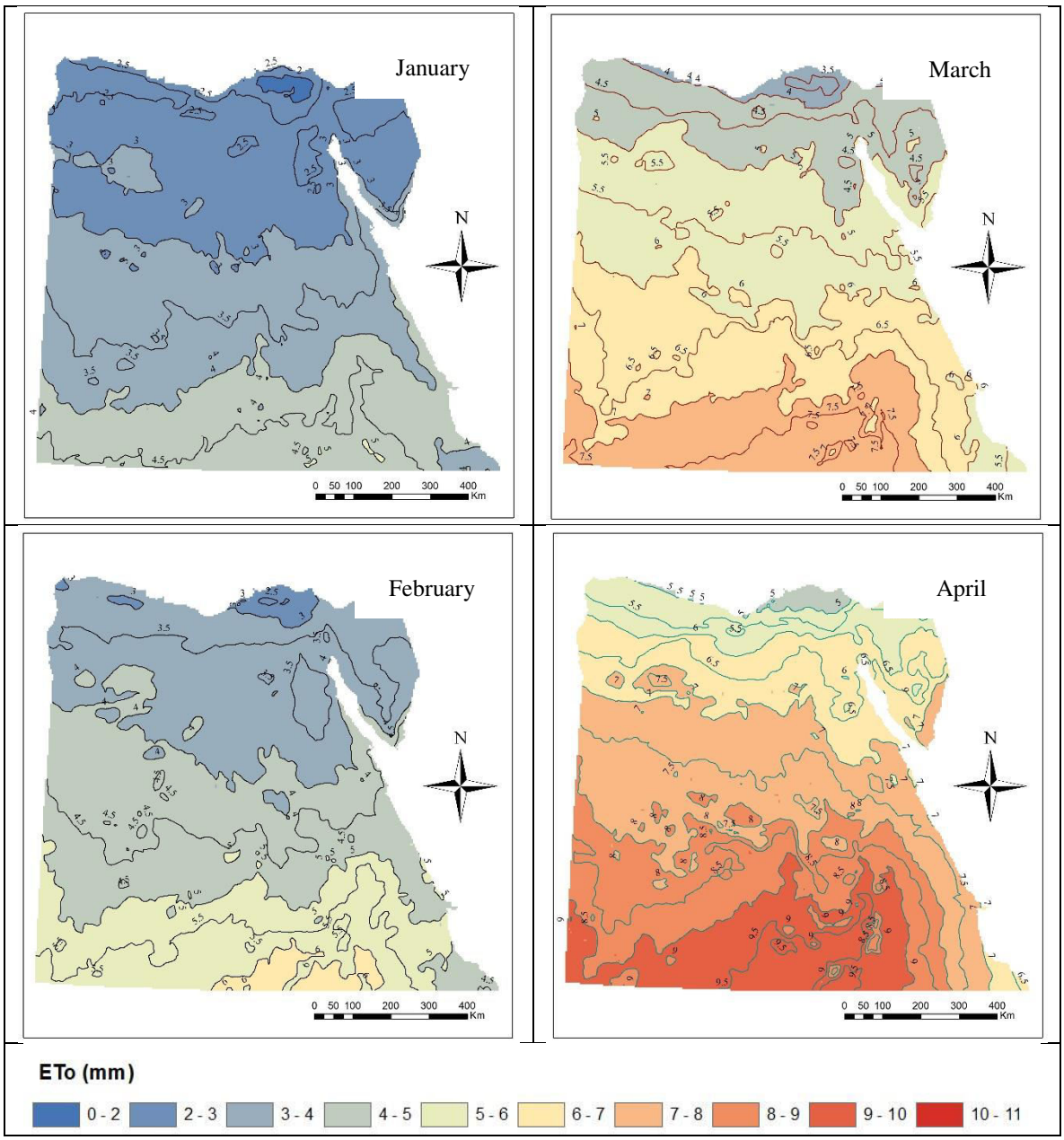

Figure-2. Egypt's average daily ETo by month for months January to April.

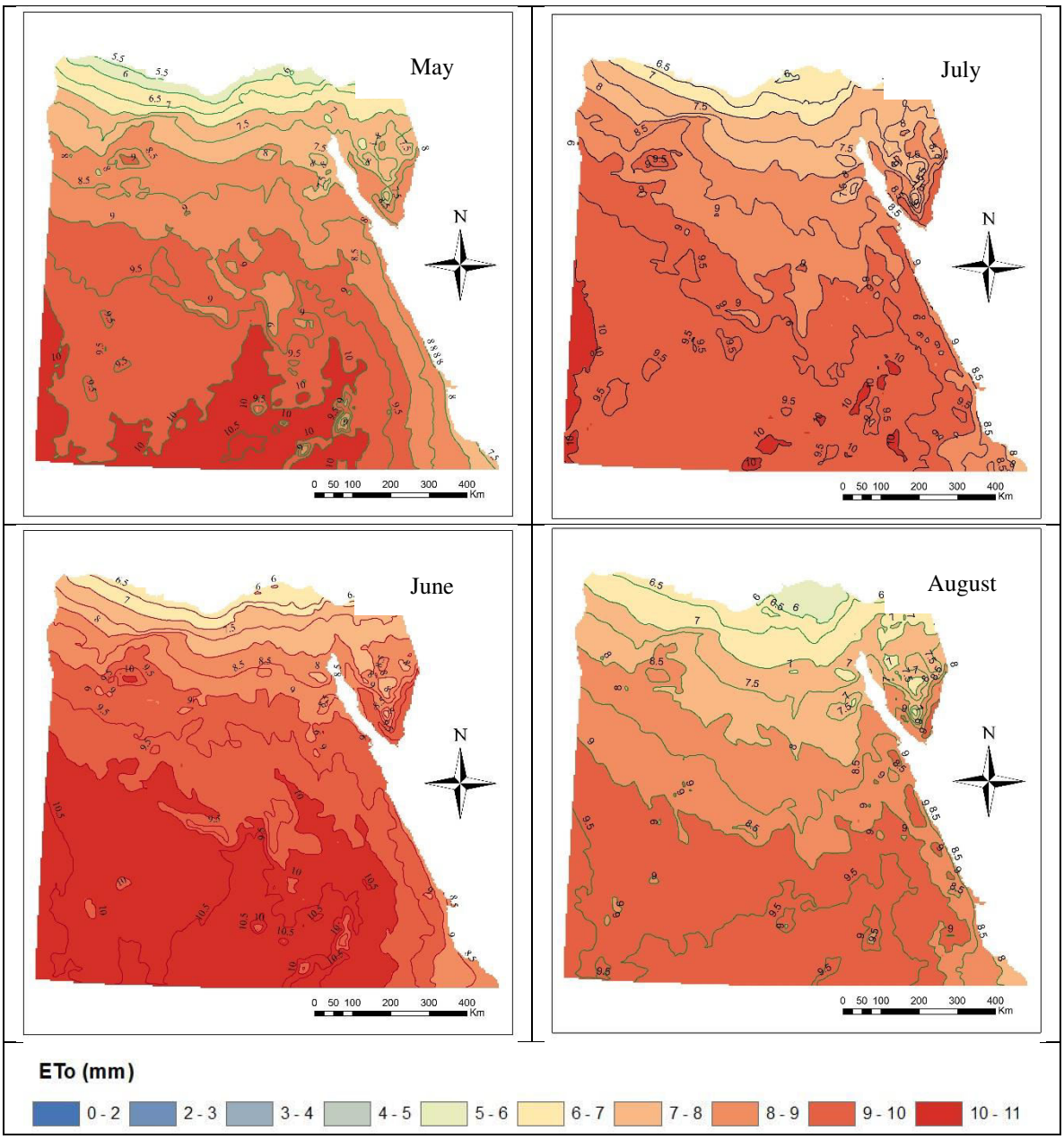

Figure-3. Egypt's average daily ETo by month for months May to August.

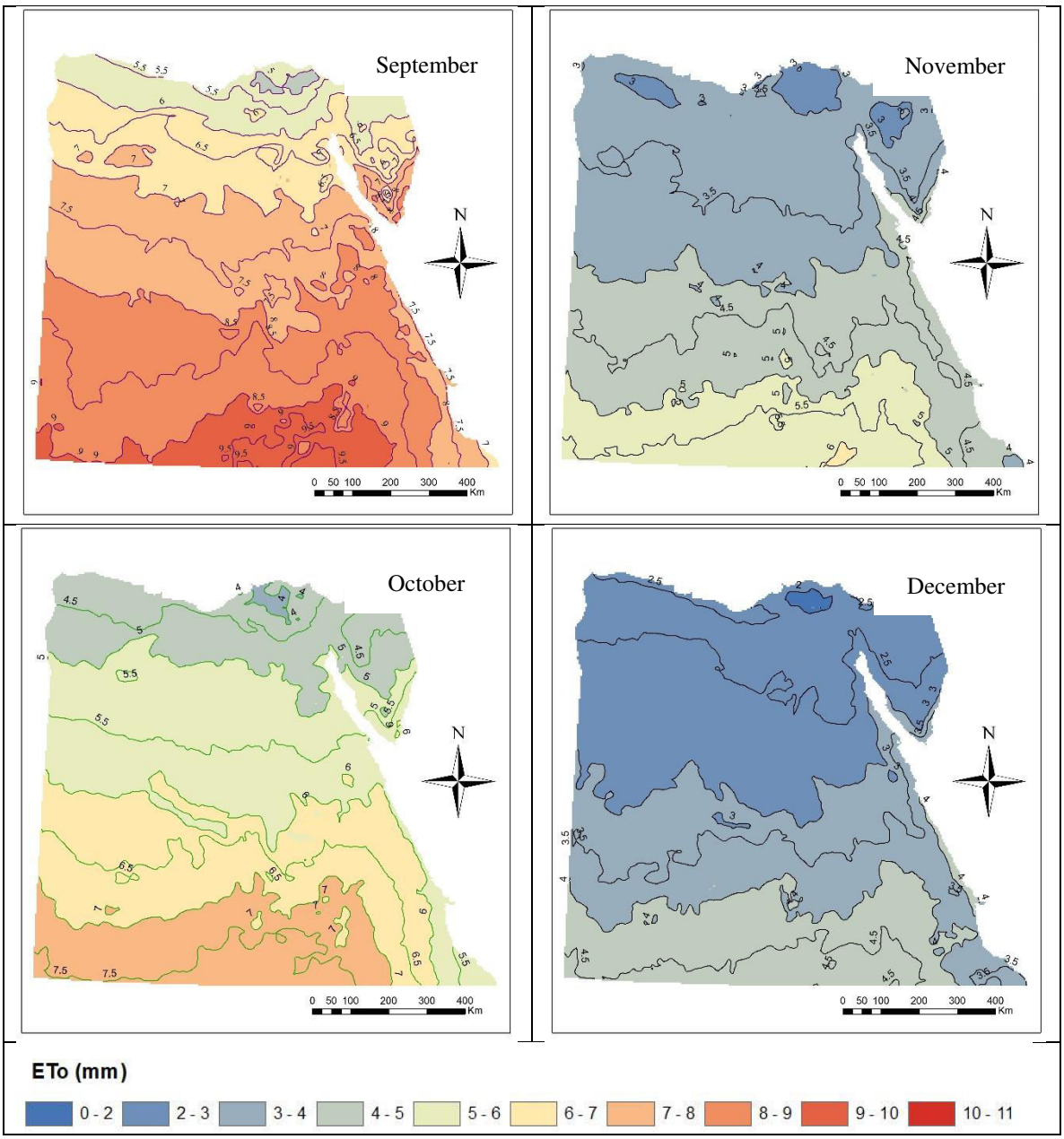

Figure-4. Egypt's average daily ETo by month for months September to December.

From Figure-2, Figure-3, and Figure-4 it is shown that the highest values of the ETo occur in summer season (June, July, and August) while the lowest values occur in winter season (December, January, and February). In addition, for all months the ETo increases from North to South and this is due to the increment of temperature and solar radiation towards the South. Moreover, the Eastern region of Egypt (Red Sea Coast) has lower values of ETo compared to middle and Western regions due to the higher values of humidity.

Statistical analysis

In order to provide more description and have better understanding for the calculated ETo values, some descriptive statistical metrics were used to give a short summary about the calculated data. The metrics used were divided into two different categories, first the measures of the central tendency of the data category, that was used in order to show the central position of the calculated ETo values, where mean and median were calculated. The second category includes the variability measures, where standard deviation, minimum, maximum, skewness coefficient and kurtosis coefficient were calculated. Table-1 shows the statistical metrics value for the ETo over the 12 months.

From Table-1 it is shown that the ETo has the least mean value in December which is about 3.28 mm, while the highest mean value occurs in June and equal to 9.5 mm. Also the median values show the same pattern for the 12 months. Regarding the variability of the ETo values the standard deviation show close values for the 12 months, while the range seem to be wider during April,

May, and June compared to January and December. For skewness, months January, February, October, November, and December shows positive skewness behaviour with a small value of skewness coefficient, less than 0.5, so it can be described as a fairy symmetrical data. The remaining month shows a negative skewness behaviour, but with distinct values, March, April and September have small skewness value greater than -0.5, so it can be described as a fairy symmetrical data, while May and August shows a moderate skewness behaviour with a values between -0.5 and -1, for June and July skewness is less than -1, so they are the highly skewed months.

The kurtosis coefficient usually refers to the combined weight of the two tail of the distribution relative to the rest of the distribution. When the kurtosis value is equal or very close to zero, the distribution is assumed to be normal, while a negative value refers to a light tail distribution and a positive value refers to a heavy tail distribution. Regarding the ETo values, most months seem to have a light tail distribution with a negative kurtosis value, while June and July show a heavier tail distribution, and May is the closest one to be normal.

Figure-5 presents the box plot for the ETo values for the 12 months over Egypt, where the minimum value, first quartile, median, third quartile, and the maximum value can be seen. In addition, the skewness can be shown for most of months. Moreover, the plot shows that January, February, November, and December have the most tightly ETo values compared to the other months. Figure-6 presents the probability density function for the twelve different months, showing the distribution shape and the skewness for each month.

Table-1. Descriptive statistical analysis of the calculated ETo.

		Jan	Feb	Mar	Apr	May	Jun	Jul	Aug	Sep	Oct	Nov	Dec
Measures of Central Tendency	**Mean**	3.41	4.43	5.93	7.66	8.86	9.50	8.96	8.50	7.67	5.96	4.18	3.28
	Median	3.23	4.34	5.94	7.70	9.07	9.79	9.25	8.80	7.80	5.94	4.11	3.11
Measures of Variability	**Standard Deviation**	0.73	0.83	1.01	1.20	1.14	1.07	0.94	1.00	1.10	0.97	0.83	0.74
	Kurtosis	-1.02	-0.83	-0.77	-0.64	0.08	0.55	0.30	-0.36	-0.68	-0.95	-0.99	-1.09
	Skewness	0.28	0.19	-0.08	-0.27	-0.87	-1.10	-1.05	-0.77	-0.38	0.04	0.32	0.34
	Minimum	1.78	2.42	3.28	4.49	5.35	5.91	5.95	5.67	4.81	3.80	2.63	1.83
	Maximum	5.05	6.32	8.01	9.90	10.64	11.06	10.44	9.99	9.82	7.98	6.16	4.93
	Range	3.27	3.89	4.73	5.41	5.29	5.14	4.48	4.32	5.01	4.18	3.53	3.09

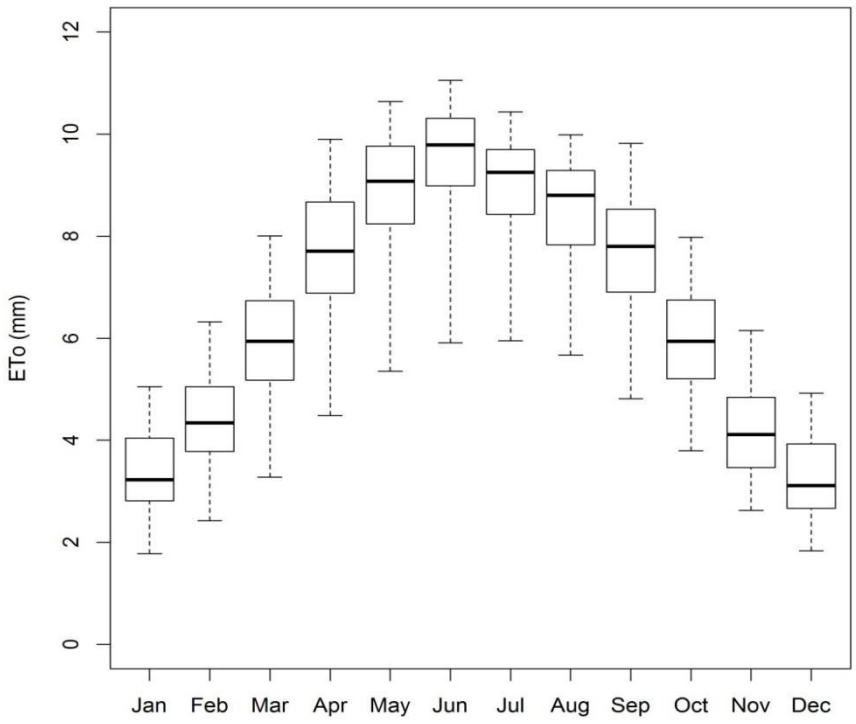

Figure-5. Boxplot for the ETo for months January to December.

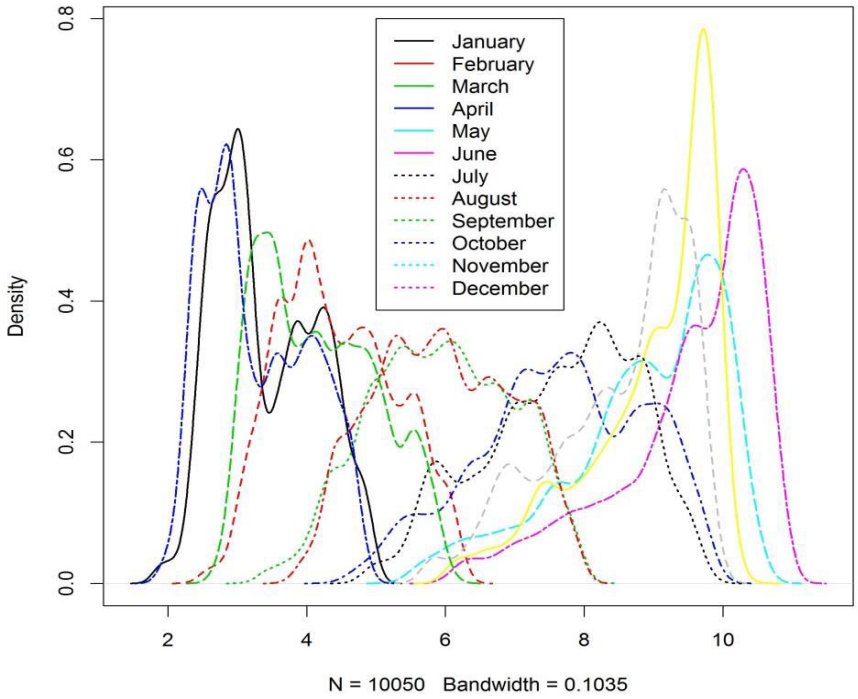

Figure-6. Plot of the PDF for the ETo for months January to December.

CONCLUSIONS

The reference evapotranspiration is calculated all over Egypt using FAO Penman Monteith equation. The climate data used for the study is monthly averaged from period 1970-2000. The ETo calculations and demonstration are done using a GIS environment. The results of ETo showed that the least mean value occurred during December which is about 3.28 mm, while the highest mean value occurred in June and equal to 9.5 mm. Also, the median values showed the same pattern for the 12 months. Regarding the variability of the ETo values the standard deviation showed close values for the 12 months, while the range seem to be wider during April, May, and June compared to January and December. The output ETo maps are useful to calculate the actual crop water requirements all over Egypt which helps in saving irrigation water due to the water scarcity situation, also the output ETo maps can be used in defining the suitable areas to be used for the future agricultural expansion, due to its low evapotranspiration values.

It is recommended to use the same methodology presented in this study but with more recently climate data in order to investigate the effect of climate change on the values of the reference evapotranspiration over Egypt, since the WorldClim Version2 used during this study was only available during the period 1970 - 2000.

REFERENCES

[1] Abou Zeid K. 2002. Egypt and the World Water Goals, Egypt's statement in Johannesburg and beyond: The 2002 World Summit on Sustainable Development and the Rise of Partnership.

[2] El-Shirbeny M. A., Ali A. E. M. and Saleh N. H. 2014a. Crop water requirements in Egypt using remote sensing techniques. Journal of Agricultural Chemistry and Environment. 3(02): 57.

[3] Yin Y., Wu S., Zheng D. and Yang Q. 2008. Radiation calibration of FAO56 Penman–Monteith model to estimate reference crop evapotranspiration in China. Agricultural water management. 95(1): 77-84.

[4] El-Shirbeny M. A., Aboelghar M. A., Arafat S. M. and El-Gindy A. G. M. 2014b. Assessment of the mutual impact between climate and vegetation cover using NOAA-AVHRR and Landsat data in Egypt. Arabian journal of geosciences. 7(4): 1287-1296.

[5] Zhao S. H., Yang Y. H., Zhang F., Sui X. X., Yao Y.J., Zhao N., Zhao Q. and Li C.Q. 2015. Rapid evaluation of reference evapotranspiration in Northern China. Arabian Journal of Geosciences. 8(2): 647-657.

[6] Smith M., Kivumbi D. and Heng L. K. 2002. Use of the FAO CROPWAT model in deficit irrigation studies. In Deficit irrigation practices. 22: 17-27.

[7] Snyder R. L., Orang M., Bali K. and Eching S. 2004. Basic irrigation scheduling BIS.

[8] Eid H. M., El-Marsafawy S. M. and Ouda S. A. 2006. Assessing the impact of climate on crop water needs in Egypt: the CROPWAT analysis of three districts in Egypt. CEEPA Discussion Papers. 29, pp. 1-35.

[9] Khalil F., Ouda S. A., Osman N. and Ghamis A. 2011, May. Determination of agro-climatic zones in Egypt using a robust statistical procedure. In Fifteenth international water technology conference. IWTC-15, Alexandria, Egypt.

[10] Ismail M. 2012. Using remote sensing and GIS application in agro-ecological zoning of Egypt. Int J Environ Sci. 1(2): 58-94.

[11] Khalil A. A. 2013. Effect of climate change on evapotranspiration in Egypt. Researcher. 5(1): 7-12.

[12] Noreldin T., Ouda S. and Amer A. 2016. Agro-climatic zoning in Egypt to improve irrigation water management. Journal of water and land development. 31(1): 113-117.

[13] Ouda S. 2015. Major crops and water scarcity in Egypt: irrigation water management under changing climate. Springer.

[14] Zohry A. and Ouda S. 2015. Management of crops intensification in Egypt to overcome water scarcity. Glob J Adv Res. 2(12): 1-7.

[15] Morsy M., El-Sayed T. & Ouda S. A. 2016. Potential evapotranspiration under present and future climate. In Management of Climate Induced Drought and Water Scarcity in Egypt (pp. 5-25). Springer, Cham.

[16] Ouda S. A. and Norledin T. A. 2017. Evapotranspiration data to determine agro-climatic zones in Egypt. Journal of water and land development. 32(1): 79-86.

[17] Monteith J. L. 1965. Evaporation and environment. The state and movement of water in living organisms. Symposium of the society of experimental biology. 19: 205-234.

[18] Allen R. G., Pereira L. S., Raes D. and Smith M. 1998. Crop evapotranspiration-Guidelines for computing crop water requirements-FAO Irrigation and drainage paper 56. Fao, Rome. 300(9): D05109.

[19] Fick S. E. & Hijmans R. J. 2017. WorldClim 2: new 1-km spatial resolution climate surfaces for global land areas. International Journal of Climatology. 37(12): 4302-4315.

[20] Takaku J. & Tadono T. 2017. Quality updates of AW3D'global DSM generated from ALOS PRISM. In Geoscience and Remote Sensing Symposium (IGARSS), 2017 IEEE International (pp. 5666-5669). IEEE.